LAWRENCE
LIVERMORE
NATIONAL
LABORATORY

LLNL-TR-700047

Structure And Mobilities Of Tungsten Grain Boundaries Calculated From Atomistic Simulations

T. Frolov, R. E. Rudd

August 9, 2016

Disclaimer

This work performed under the auspices of the U.S. Department of Energy by Lawrence Livermore National Laboratory under Contract DE-AC52-07NA27344.

STRUCTURE AND MOBILITIES OF TUNGSTEN GRAIN BOUNDARIES CALCULATED FROM ATOMISTIC SIMULATIONS — Timofey Frolov and Robert E. Rudd (Lawrence Livermore National Laboratory)

OBJECTIVE

The objective of this study is to develop a computational methodology to predict structure, energies and mobilities of tungsten grain boundaries as a function of misorientation and inclination. The energies and the mobilities are the necessary input for thermomechanical model of recrystallization being developed by the Marian Group at UCLA.

SUMMARY

Recrystallization determines the upper extent of the operating temperature of tungsten as a divertor or first-wall material. At temperatures above the onset of recrystallization, migrating grain boundaries sweep out defects that contribute to hardening. These processes make the recrystallized material unsuitable because of its brittleness. Thermomechanical models to predict recrystallization and its effect on mechanical properties have to be informed of the mechanisms of grain boundary migration under stress and other driving forces at tokamak operating temperatures. Recent experimental and computational studies suggest that addition of impurities and elevated temperatures can trigger structural transformations at grain boundaries that result in orders of magnitude increase in mobility. Here we present preliminary results demonstrating that tungsten grain boundaries do exhibit phase transformations and calculate the mobilities needed for thermomechanical models of recrystallization.

BACKGROUND

Tungsten has been identified as the divertor material in ITER and is a leading candidate for the plasma-facing components in DEMO and subsequent magnetic fusion energy systems because of its high thermal conductivity, high melting point, high mechanical strength at elevated temperature, and low sputtering yield. While tungsten has a number of favorable properties it is also intrinsically brittle even at relatively high temperatures especially after recrystallization. As metals are subjected to harsh conditions, their microstructures change leading to changes in materials properties. Defects build up in the metal, increasing its strength, but grain boundary motion at high temperature can sweep up the defects and produce relatively pristine, recrystallized material. Recrystallization typically sets the upper operating temperature of tungsten, affecting the performance of the fusion energy system. The need for predictive models of material behavior at first-wall and divertor conditions motivates the development of computational models and simulations that can predict mechanical and kinetic properties of tungsten grain boundaries. Recent experimental and computational studies in materials like copper demonstrated that elevated temperatures and changes in chemical composition can lead to structural transformations at grain boundaries that result in discontinuous changes in materials properties [1, 2]. Experimental studies linked this kind of transition to abnormal grain growth and embrittlement in metallic and ceramic systems [3-5]. Here we use atomistic simulations to understand the role of grain boundaries in plasticity including grain boundary mobility, which affects recrystallization, and the interaction of dislocations with the grain microstructure, which is an important part of the embrittlement problem.

PROGRESS AND STATUS

Methods

Mobilities of tungsten grain boundaries can be calculated directly from atomistic simulations of shear stress driven grain boundary motion. Shear stress applied parallel to the grain boundary plane induces grain boundary migration [6]. The deformation of a bicrystal after coupled grain boundary motion is

illustrated in Figure 1a. The portion of a crystal swept by the boundary is sheared as indicated by vertical dashed line. Coupled grain boundary motion is characterized by a coupling factor, β, which is a ratio of the tangential and normal grain boundary velocities. For relatively low-angle boundaries the mechanism of coupled motion can be explained by examining the collective motion of grain boundary dislocations. When shear stress is applied to a bicrystal these dislocations move in response to the Peach-Koehler force. Figure 1b schematically illustrates grain boundary dislocations before and after coupled motion. The collective motion of grain boundary dislocations results in normal grain boundary displacement and tangential translations of the grains relative to each other. The coupling is called perfect when β is just determined by the bicrystal geometry. Based on the mechanism illustrated in Figure 1b coupling factor can be calculated as

$$\beta = 2 \tan(\theta/2) \qquad (1)$$

where θ is the misorientation angle across the boundary. Symmetries present in a crystal can result in multiple coupling modes, each characterized by a different coupling factor. (100) symmetrical tilt boundaries with θ closer to 0° couple in the <100> mode, while grain boundaries with θ closer to 90° couple in the <110> mode.

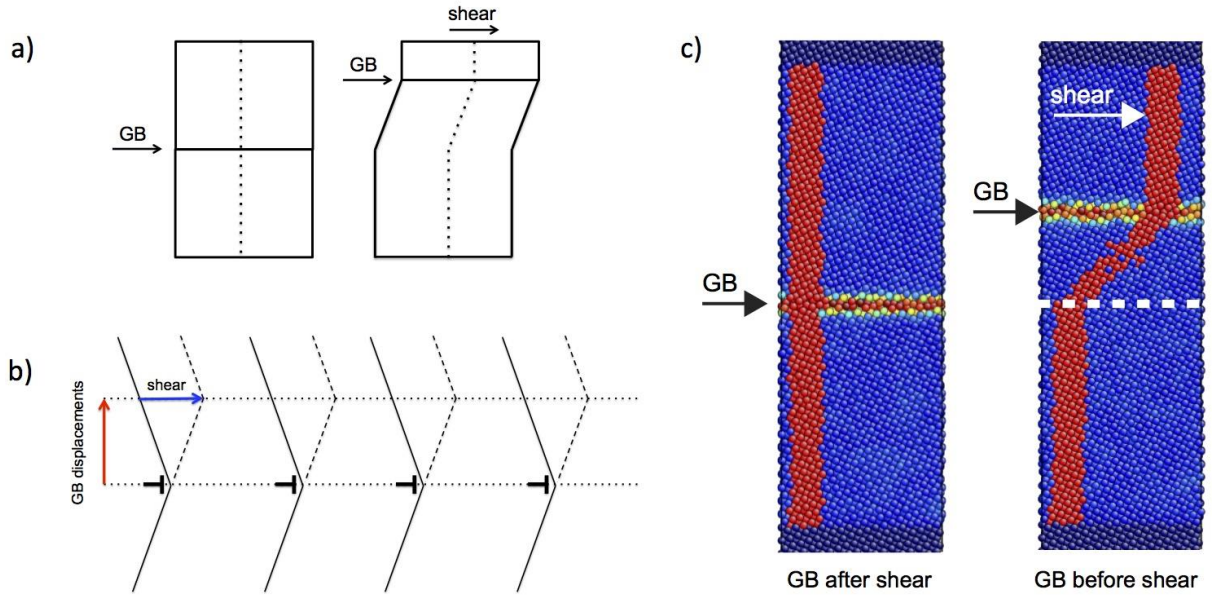

Figure 1. a) Bicrystal shear deformation produces grain boundary migration b) Mechanism of coupled motion due to the collective motion of grain boundary dislocations. c) Atomistic simulations of grain boundary coupled motion.

In the linear mobility regime relevant to recrystallization, the grain boundary velocity v_{GB} is proportional to the driving force F as $v_{GB} = MF$, where M is the grain boundary mobility. It can be shown that the driving force for coupled motion is proportional to shear stress $F=\sigma\beta$, so that the velocity is given by

$$v_{GB} = M\ \sigma\beta. \qquad (2)$$

Grain boundary velocity, shear stress and the coupling factor can be calculated from atomistic simulations of coupled motion. Thus, Eq. (2) allows predictions of grain boundary mobility.

Molecular dynamics (MD) simulations of tungsten grain boundaries were performed using the Large-scale Atomic/Molecular Massively Parallel Simulator (LAMMPS) software package [7]. The interactions between atoms were modeled using a tungsten EAM potential [8]. We modeled high-angle Σ5(310)[001] and low-angle Σ(978)[11-2] symmetrical tilt boundaries with and without defects present. Σ5(310)[001] is a typical high angle boundary with misorientation angle of 36.87°. The dimensions of the bicrystals were $25 \times 3 \times 12$ nm^3. The simulation block contained 60000 atoms. The low-angle boundary has a misorientation angle of 11°, with the grains rotated around the [11-2] tilt axis. The bicrystal with dimensions $10 \times 10 \times 30$ nm^3 contained 223000 atoms. Both bicrystals had the tilt axis parallel to the *y* direction, and grain boundary planes normal to the *z* direction. Periodic boundary conditions were applied in the *x* and *y* directions, while fixed boundary conditions were used in the *z* direction to impose shear deformation.

Equilibrium boundary structures were obtained by sampling rigid translations of grains relative to each other followed by static relaxations. Figure 2a illustrates the structure of the Σ5(310)[001] boundary composed of kite-shaped structural units. The structure of the low-angle boundary is represented by a periodic array of 1/2<111> edge dislocations (Figure 3a). The bicrystals were used to perform simulations of coupled motion at temperatures ranging from 500K to 2500K. During the simulations the atoms inside the 10Å thick region at the bottom of the simulation block were kept fixed, while the 10Å thick layer of atoms at the top of the block were moved with a constant velocity of 0.1 m/s in the x direction. The atoms in the middle of the block were simulated using the canonical (NVT) ensemble with Nose-Hoover thermostat.

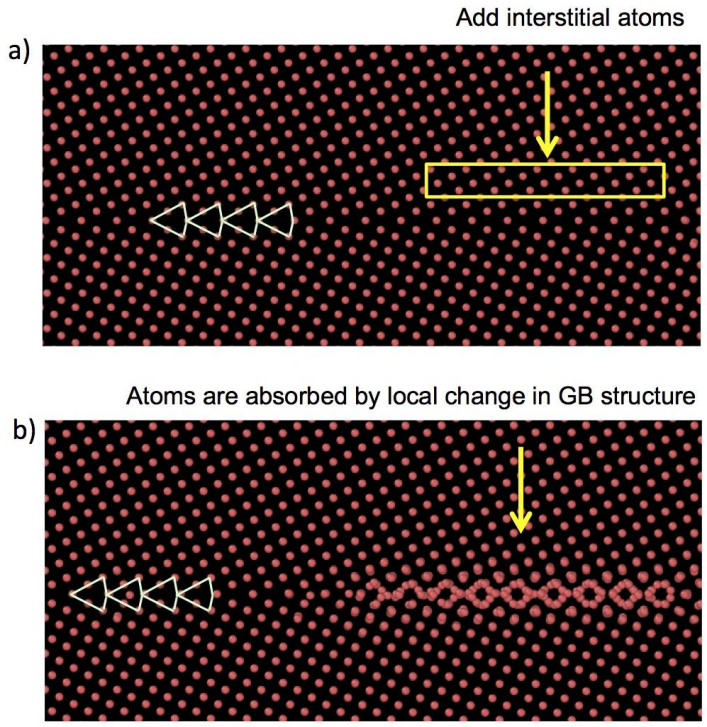

Figure 2. a) Structure of Σ5(310)[001] symmetrical tilt boundary in W composed of kite-shaped structural units. b) Grain boundary absorbs interstitial atoms by undergoing a structural transformation.

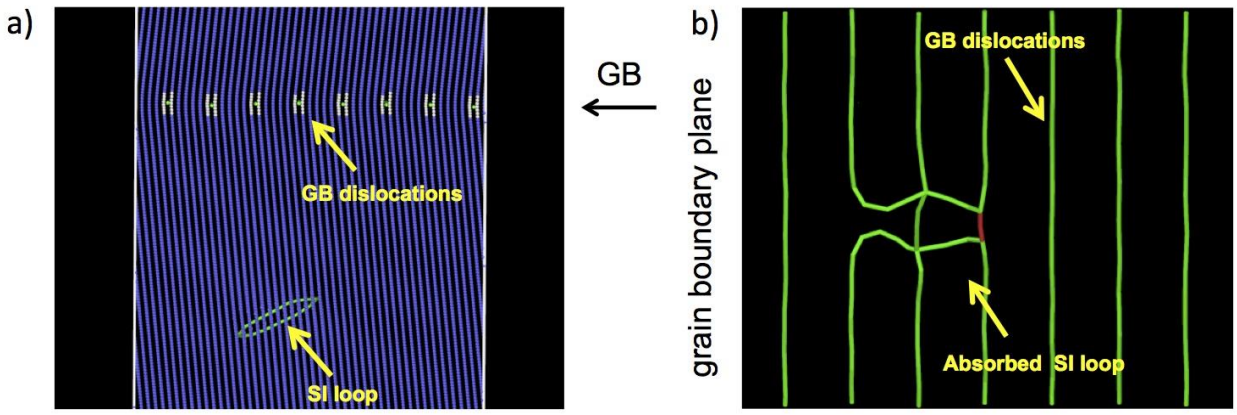

Figure 3. a) Structure of Σ (978)[11-2] symmetrical tilt boundary in W composed of 1/2<111> edge dislocations. b) Grain boundary structure after interstitial loop was absorbed.

Figure 1c illustrates a bicrystal after 30 ns of the coupled motion. The initial positions of the grain boundaries are indicated by the white dashed lines. The deformation of the bicrystal revealed by the atomistic simulations is consistent with the schematic picture in Figure 1a. The red column of marker atoms clearly demonstrates that the region swept by the boundary is sheared. The coupling factor β can be obtained directly from MD simulations by calculating the ratio of upper grain displacement and the grain boundary normal displacement. The ideal coupling factor predicted by Eq. (1) was calculated from MD simulation for both high and low-angle boundaries.

Point Defects

In the presence of high temperature, impurities and point defects, grain boundary structure and mobility can change significantly. Recent experimental studies in ceramics indicate that such transformations can change grain boundary mobility by orders of magnitude producing pronounced changes in microstructure evolution [2, 9]. To quantify the possible effect of lattice defects on grain boundary mobility, we investigate how these grain boundaries interact with interstitials and self-interstitial loops.

High-angle boundary

In the case of the high-angle boundary individual interstitial atoms were randomly injected inside a rectangular region above the boundary as indicated in Figure 2a. The bicrystal with defects was then annealed for 100ns at T=2000K. During the first several nanoseconds the interstitials diffuse to the boundary and produce noticeable reconstruction of the kite-shaped structural units. These reconstructed regions agglomerate during the later times and form a patch with a different grain boundary structure, which is illustrated in Figure 2b. Throughout the simulation the newly formed patch coexists with the original structure while atoms diffuse within the boundary. This transformation of the grain boundary structure is consistent with recent results in Cu that demonstrated multiple grain boundary states characterized by different atomic densities [10]. Atomistic simulations allow evaluation of the mobilities of the two structures, as well as the mobility of the “damaged” boundary that has two different grain boundary structures present simultaneously.

Low-angle boundary

1/2<111> interstitial loops are formed in tungsten divertors as a result of radiation damage. A single interstitial loop with diameter ranging from 10 to 50 Å was introduced inside one of the crystals in a simulation block with the 11° boundary as illustrated in Figure 3a. During subsequent isothermal annealing the loop glides towards the boundary driven by the elastic interaction and gets absorbed. The structure of the grain boundary dislocation network with the interstitial loop absorbed is illustrated in Figure 3b. The boundary is composed of 1/2<111> edge dislocations, and one segment of the loop gets annihilated upon absorption. The red segment in the figure indicates that the Burgers vector doubled. This configuration represents a boundary with a circular step and has dislocation lines that are not parallel to the tilt axis.

To evaluate the effect of loop absorption on grain boundary mobility, we performed the simulations of coupled motion of defective grain boundaries. When shear stress is applied to the bicrystal, the network of 1/2<111> dislocations at the grain boundary illustrated in Figure 3b moves in a manner consistent with perfect coupling. In other words, the absorbed interstitial loop does not change the mechanism of grain boundary motion. Figure 4 illustrates shear stress during coupled motion at 500K for one clean boundary and two boundaries with interstitial loops with diameter of 25Å and 50Å. Higher average and peak stresses are required to move the boundaries with loops, suggesting that mobility of the boundary decreased and the shear strength of the bicrystal is increased due to the loop absorption.

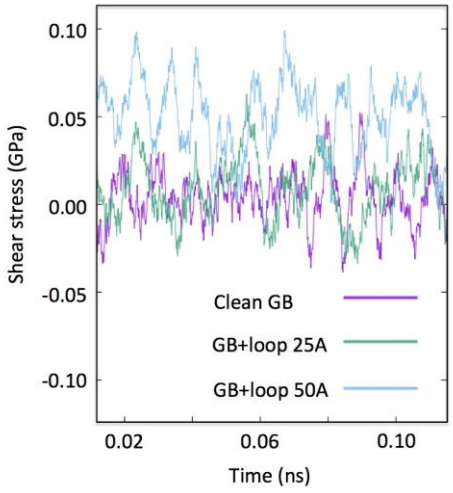

Figure 4. Shear stress during coupled motion at 500K for one clean boundary and two boundaries with interstitial loops with diameter of 25 Å and 50 Å. Higher average and peak stress is required to move the boundaries with larger loops, indicating that mobility of the boundary decreased due to the loop absorption.

Summary and future studies

In summary, we performed simulations of coupled motion of two representative high- and low-angle grain boundaries. Atomistic simulations give direct access to shear stress during grain boundary migration, predict the coupling factor β and grain boundary velocity. This information has been used to calculate grain boundary mobility. In addition to modeling of pristine or undamaged boundaries, we also investigated the effect of interstitial absorption on grain boundary structure and mobility. Low- and high-angle boundaries displayed different mechanisms of defect absorption. While the damaged low-angle

boundary can be described as a network of 1/2<111> edge dislocations, high-angle boundary absorbs atoms by undergoing structural transformation. Absorption of defects has strong effect on grain boundary mobility and increases the shear strength of the material. Systematic calculation of grain boundary energies and mobilities as function of misorientation and inclination will be the subject of future work. These results will provide necessary input parameters for thermomechanical model of recrystallization under development by the Marian group at UCLA. Direct experimental measurement of the predicted high-temperature grain boundary structures and velocities is not feasible with existing technology, so we rely on comparison of the thermomechanical model with experiment for validation.

Acknowledgments

This work was performed under the auspices of the U.S. Department of Energy by Lawrence Livermore National Laboratory under Contract No. DE-AC52-07NA27344.

References

[1] T. Frolov, M. Asta, and Y. Mishin, Current Opinion in Solid State and Materials Science (2016).
[2] P. R. Cantwell, M. Tang, S. J. Dillon, J. Luo, G. S. Rohrer and M. P. Harmer, Acta Materialia 62, 1 (2014).
[3] S. J. Dillon and M. P. Harmer, Acta Materialia 55, 5247 (2007).
[4] J. Luo, H. Wang, and Y.-M. Chiang, Journal of the American Ceramic Society 82, 916 (1999).
[5] J. Luo, H. Cheng, K. M. Asl, C. J. Kiely, and M. P. Harmer, Science 333, 1730 (2011).
[6] J. W. Cahn, Y. Mishin, and A. Suzuki, Acta Materialia 54, 4953 (2006).
[7] S. Plimpton, Journal of Computational Physics 117, 1 (1995).
[8] X. W. Zhou, R. A. Johnson, and H. N. G. Wadley, Physical Review B 69, 144113 (2004).
[9] T. Frolov, Applied Physics Letters 104, (2014).
[10] T. Frolov, D. L. Olmsted, M. Asta, and Y. Mishin, Nature Communications 4, 1899 (2013).